



This document was prepared for the ETI by third parties under contract to the ETI. The ETI is making these documents and data available to the public to inform the debate on low carbon energy innovation and deployment.

**Programme Area:** Marine

**Project:** PerAWAT

**Title:** Design and Specification of Ducted Disc Experiments

---

### Abstract:

Simulations elsewhere in the project indicate that a rotor within a duct of outer diameter  $D$  experiences lower thrust on the rotor plane than a rotor of the same diameter. Experimental evaluation of the influence of duct augmentation on performance is essential to i) provide confidence in this finding and ii) demonstrate that the PerAwaT modelling tools are relevant to the fundamental device concepts presently in development (i.e. OpenHydro AND open-centre rotors). This work package addresses the design and specification of a series of experiments to assess the validity of CFD predictions of the effect of turbine augmentation by a duct. CFD simulations are analysed to determine the range of local thrust coefficients over which a measurable performance difference is observed and appropriate disc porosities are identified. The equipment required to conduct disc, duct and rotor experiments is summarised and a sequence of tests is proposed.

### Context:

The Performance Assessment of Wave and Tidal Array Systems (PerAWaT) project, launched in October 2009 with £8m of ETI investment. The project delivered validated, commercial software tools capable of significantly reducing the levels of uncertainty associated with predicting the energy yield of major wave and tidal stream energy arrays. It also produced information that will help reduce commercial risk of future large scale wave and tidal array developments.

---

### Disclaimer:

The Energy Technologies Institute is making this document available to use under the Energy Technologies Institute Open Licence for Materials. Please refer to the Energy Technologies Institute website for the terms and conditions of this licence. The Information is licensed 'as is' and the Energy Technologies Institute excludes all representations, warranties, obligations and liabilities in relation to the Information to the maximum extent permitted by law. The Energy Technologies Institute is not liable for any errors or omissions in the Information and shall not be liable for any loss, injury or damage of any kind caused by its use. This exclusion of liability includes, but is not limited to, any direct, indirect, special, incidental, consequential, punitive, or exemplary damages in each case such as loss of revenue, data, anticipated profits, and lost business. The Energy Technologies Institute does not guarantee the continued supply of the Information. Notwithstanding any statement to the contrary contained on the face of this document, the Energy Technologies Institute confirms that the authors of the document have consented to its publication by the Energy Technologies Institute.

PerAWAT WG4 WP3 D1  
Design and specification of ducted disc experiments

Project	PerAWAT
Work package	WG4
Deliverable	WG4 WP3 D1
Responsible author	Tim Stallard,
Second reading	Richard Willden, Simon McKintosh, Tong Feng
Circulation	UoM / UoO / EdF /GH
To be approved by	Robert Rawlinson-Smith (GH)
Date	14 Sep 2012
Issue	V1

Document revision history

Issue	Date	Summary
V1.0	14Sep12	Issued to GH and ETI

## EXECUTIVE SUMMARY

Simulations by UoO (WG3WP1 and Fleming et al. 2011) indicate that a rotor within a duct of outer diameter  $D$  experiences lower thrust on the rotor plane than a rotor of the same diameter. Experimental evaluation of the influence of duct augmentation on performance is essential to i) provide confidence in this finding and ii) demonstrate that the PerAwaT modelling tools are relevant to the fundamental device concepts presently in development (i.e. OpenHydro AND open-centre rotors). This work package addresses the design and specification of a series of experiments to assess the validity of CFD predictions of the effect of turbine augmentation by a duct. CFD simulations are analysed to determine the range of local thrust coefficients over which a measurable performance difference is observed and appropriate disc porosities are identified. Seven discs and a duct have been manufactured and are either available or due for imminent delivery. In addition, two series of experiments are specified to improve confidence in performance predictions of a small-scale rotor previously employed for array scale experiments in WG4WP2 and to improve understanding of bounding surface proximity on wake structure. These experiments comprise measurement of the thrust and power curves and wake deficit of a 270 mm diameter rotor at quarter, mid- and three-quarter depth of an 800 mm deep flume. The equipment required to conduct disc, duct and rotor experiments is summarised and a sequence of tests is proposed. The specified experimental measurements are estimated to require 22 days of 'in-flume' testing and the EdF flume is available up to end November 2012 for conduct of these experiments.

## CONTENTS

<b>CONTENTS</b>	<b>III</b>
<b>1 INTRODUCTION</b>	<b>4</b>
1.1 SCOPE OF THIS DOCUMENT	4
1.2 SPECIFIC TASKS ASSOCIATED WITH WG4 WP3	4
<b>2 DATA REQUIRED</b>	<b>5</b>
2.1 DUCTED AND UNDUCTED DISC EXPERIMENTS	5
2.2 ROTOR PERFORMANCE: LOW BLOCKAGE & SHEAR	8
2.3 ROTOR WAKE: BOUNDING SURFACE PROXIMITY	8
<b>3 EQUIPMENT</b>	<b>10</b>
3.1 FLUME	10
3.2 DISC POROSITY AND GEOMETRY	10
3.3 DUCT DESIGN	11
3.4 THRUST MEASUREMENT	12
3.5 ROTOR TORQUE AND SPEED MEASUREMENT	12
3.6 FLOW MEASUREMENT	12
3.7 DATA LOGGING	13
<b>4 LOGISTICS</b>	<b>14</b>
4.1 EQUIPMENT TO DISPATCH TO EDF	14
4.2 INDICATIVE SCHEDULE OF EXPERIMENTS	15
<b>5 CONCLUSIONS</b>	<b>16</b>
<b>REFERENCES</b>	<b>17</b>
<b>APPENDIX 1: POROUS DISC DESIGNS</b>	<b>18</b>
<b>APPENDIX 2: DUCT DESIGN</b>	<b>19</b>
<b>APPENDIX 3: WAKE MEASUREMENT CO-ORDINATES</b>	<b>21</b>

# 1 INTRODUCTION

## 1.1 Scope of this document

This document constitutes the first deliverable (D1) of working group 4, work package 3 (WG4WP3) of the PerAWAT (Performance Assessment of Wave and Tidal Arrays) project funded by the Energy Technologies Institute (ETI). The project partners of this work package are University of Manchester (UoM), University of Oxford (UoO), Electricite de France (EdF) and Garrad Hassan (GH).

The majority of device scale experimental and numerical analysis within PerAWaT addresses the performance and wake of the open-blade type fundamental device concept (FDC). The intention of WG4WP3 is to obtain experimental data describing the wake and performance of the alternative device concept of a ducted device. Two further issues are also addressed that relate to all device types: the influence of channel blockage and of sheared flow on both device performance and wake recovery.

In this report, a series of experiments are described to address the effect of ducting, blockage and sheared flow on turbine performance and wake. The parameter ranges of interest and background to ducted device performance and to the influence of blockage and bounding surface proximity on rotor performance and wake structure are reviewed (Section 2). Relevant parameter ranges are identified and a summary given of required experimental measurements. Appropriate equipment and procedures summarised (Section 4). The design process includes identification of disc porosity to develop thrust coefficients over which measurable changes of performance are predicted due to ducting.

## 1.2 Specific tasks associated with WG4 WP3

### **WG4WP3D1 31 August 2012 (UoM) (postponed to 14 September 2012 due to VR start date)**

Equipment and specification delivered to EdF (UoM and UoO)  
& EdF confirm flume availability (EdF)

Acceptance: Proof of delivery and statement confirming flume availability. (EdF)

### **WG4WP3D2: 30 November 2012 (EdF)**

Experiment data, quality controlled and delivered (EdF)

Acceptance: Summary report explaining data format and QC process. Data uploaded to ftp. (EdF)

### **WG4WP3D3: 28 February 2013 (UoO)**

Report comparing experiments to CFD analysis (UoO, UoM and GH)

Acceptance: Report to include description of scope of experiments, experiment procedure and data QC process. Report will summarise findings concerning:

- 1) Experimental measurement of effect of duct on turbine performance and wake.
- 2) Extent of agreement between experiment and CFD simulations of duct turbine.
- 3) Effect of free-surface and rigid-bed proximity on rotor wake structure
- 4) Variation of power and thrust coefficient of UoM rotor in unbounded domain with comparison to GH Tidal Bladed.

## 2 DATA REQUIRED

The motivation for these experiments is to obtain experimental data quantifying:

1. Influence of turbine augmentation with duct on turbine performance and on wake structure. Improves confidence in the application of wake models to ducted devices.
2. Performance and wake of the rotor employed in WG4WP2 in unconstrained flow. This allows direct comparison of GH Tidal Bladed predictions to measurements with UoM rotor. Increases confidence in the effect of blockage measured in WG4 WP2.
3. The effect of bounding surface proximity on the form of an open-bladed turbine wake.

The following briefly describes the motives for each set of experiments, and summarises the required experiment configurations and outputs. Equipment to conduct the experiments is documented in Section 3.

### 2.1 Ducted and Unducted Disc Experiments

Experimental measurements are required to quantify the discrepancy between performance of an open-bladed (unducted) turbine and a ducted turbine. Key parameters to measure are thrust coefficient and power coefficient both without and with a duct. Three performance metrics are employed:

$$\text{- Global thrust coefficient: } C_T = F_x / (1/2\rho A_D U_0^2) \quad \text{Eq.1}$$

$$\text{- Local thrust coefficient: } c_x = F_x / (1/2\rho A_D U_D^2) \quad \text{Eq.2}$$

$$\text{- Effective power coefficient: } C_P = F_x U_D / (1/2\rho A_D U_0^3) \quad \text{Eq.3}$$

Where  $U_0$  denotes velocity of the ambient flow averaged across the rotor plane and  $U_D$  the velocity across the disc. A rotor designed for operation without a duct will be different from a rotor designed for operation within a duct and so limited knowledge will be gained from studying a single rotor without and with a duct. Instead it is proposed that the effect of a duct on porous disc thrust and wake is investigated. Direct comparison can then be drawn between experimental measurements of a porous disc and numerical simulations of an actuator disc.

CFD simulations of an actuator disc without and with a duct demonstrate that, for comparable blockage, effective power coefficient of a disc of diameter  $D_1$  is typically reduced if augmented with a duct of outer diameter  $D_0 > D_1$ . It is known that the thrust coefficient and effective power coefficient of any turbine is dependent on the channel blockage ratio, defined by the ratio of projected outer area and vertical channel area,  $A_D/A_C$ . Therefore care must be taken to compare ducted and unducted turbines at similar blockage ratios. From a range of eight geometries a duct with outer diameter  $D_0 = 1.14D_1$  has been found to provide the most effective balance of power coefficient and basin efficiency (Fleming et al. 2011). Linear momentum considerations indicate that the difference of  $C_T$  between these two due to blockage is less than 5% if  $A_1/A_C < 6.4\%$  (i.e.  $dC_T = (1-A_0/A_C)^{-2} / (1-A_1/A_C)^{-2} < 1.05$  for  $A_C > 15.4 A_1$ ) and less than 1% for  $A_1/A_C < 3\%$ .

RANS CFD simulations have been conducted for the following geometries located at the centre of a channel cross-section of 1.5 m width and 0.8 m depth ( $A_C = 1.2 \text{ m}^2$ ):

- i) Disc diameter  $D_1 = 270 \text{ mm}$ ,  $A_1/A_C = 4.8\%$ ,
- ii) Disc diameter  $D_0 = 311 \text{ mm}$ ,  $A_0/A_C = 6.3\%$
- iii) Disc diameter  $D_1$  within duct of outer diameter  $D_0$ ,  $A_D/A_C = 6.3\%$ .

The two discs exhibit similar power and thrust variation (Figure 2.1) confirming that the effect of channel blockage is small. For low values of thrust coefficient the ducted disc attains higher power coefficient whereas at high thrust coefficient, power coefficient is reduced markedly.

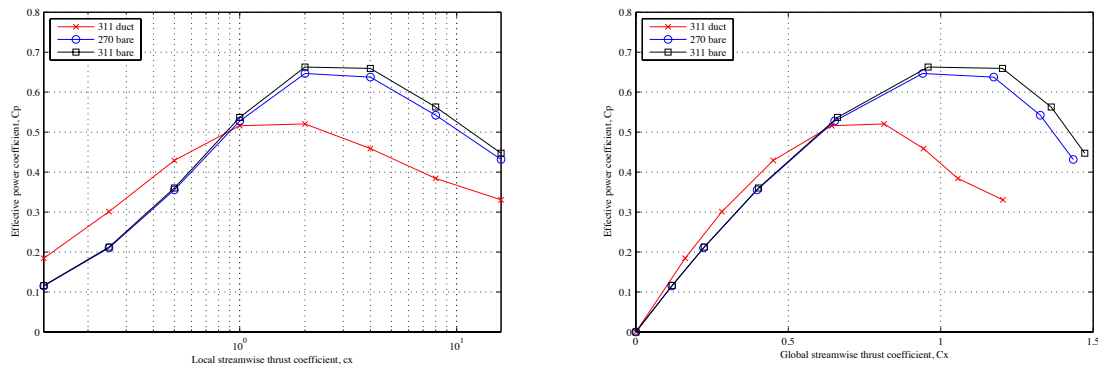


Figure 2.1: RANS CFD prediction of variation of effective power with local and global thrust coefficient for unducted discs of blockage 4.8%, and 6.3%

Experimental data is required for comparison to Figure 2.1. Three ranges of local thrust coefficient are of particular interest:  $c_x < 0.9$  for which the ducted disc develops higher CP than both discs for equivalent  $c_x$ ,  $c_x \sim 0.9$  for which the CP of both duct and discs are similar and  $0.9 < c_x < 10$  for which the bare discs develop higher CP than the ducted disc. Experimental data is therefore required for at least five  $c_x$  values as listed in Table 2.1.

**Table 2.1x:** Test List for porous disc and ducted porous disc experiments

Test No.	Configuration		CFD Predictions		Fx	Velocity			
	Disc	Duct	CT	Cx		X	Ypos	Zpos	Nu
1.11	270	n/a	0.40	0.50	Y	L/2	0	Zpts-A	8
1.12	270	n/a	0.65	0.9	Y	L/2	Ypts-A	Zpts-A	15
1.13	270	n/a	0.8	2.0	Y	L/2	0	Zpts-A	8
1.14	270	n/a	1.0	10.0	Y	L/2	Ypts-A	Zpts-A	15
1.15	270	n/a	> 1.0	>10.0	Y	L/2	0	Zpts-A	8
1.16	270	n/a	0.8	2.0	Y	2-12D	0	0	6
1.17	270	n/a	1.0	10.0	Y	2-12D	0	0	6
1.21	270	311	0.40	0.50	Y	L/2	0	Zpts-A	8
1.22	270	311	0.65	0.9	Y	L/2	Ypts-A	Zpts-A	15
1.23	270	311	0.8	2.0	Y	L/2	0	Zpts-A	8
1.24	270	311	1.0	10.0	Y	L/2	Ypts-A	Zpts-A	15
1.25	270	311	> 1.0	>10.0	Y	L/2	0	Zpts-A	8
1.26	270	311	0.8	2	Y	2-12D	0	0	6
1.27	270	311	1.0	10.0	Y	2-12D	0	0	6
1.28	n/a	311	0	0	Y	L/2	0	0	1
1.31	311	n/a	0.8	2	Y	L/2	0	Zpts-A	8
1.32	311	n/a	1	10	Y	L/2	0	Zpts-A	8

**Note:** velocity at each X,Y,Z ordinate to include 1 No. 5 min sample or 3 No. 1 min samples.

**Note:** co-ordinates for traverses Ypts-A, Zpts\_A are given in Appendix 3.

For direct comparison to Figure 2.1, either power output (CP) and thrust or, thrust and velocity across the turbine plane are desirable. Several methods are available to measure net thrust but there are

practical constraints to measurement of either power or velocity across the turbine. Power output may be measured if a rotor is employed and this approach was employed in WG4WP2. However, rotor design for use within a duct differs from an open-bladed turbine (see WG4WP1D2). Use of a rotor would therefore limit comparison and so motivates the use of porous discs. Measurement of velocity across the disc, or within the duct, is not practical since the instrument will disturb the flow. An alternative is to estimate disc velocity from measurement of thrust or velocity immediately downstream of the rotor. Global thrust coefficient,  $C_T$ , follows from measured thrust by Eq.1. Assuming that disc velocity is uniform (see Figure 2.2) and that the magnitude of local thrust coefficient is independent of disc velocity,  $c_x$ , can be estimated from  $C_T$  by linear momentum theory. This leads to the following estimates of disc velocity and power coefficient:

$$U_{D,est}, \text{ disc velocity estimated:} \quad U_{D,est} \sim [F_x / (1/2\rho A_D c_x)]^{1/2} \quad \text{Eq. 4}$$

$$C_{P,est}, \text{ power coefficient estimated:} \quad C_P = F_x U_{D,est} / (1/2\rho A_D U_0^3) \quad \text{Eq. 5}$$

Based on CFD predictions of force only, Equation 5 yields power coefficients to within 2% of the CFD predictions of power (Figure 2.3). For these simulations, pressure drop across the actuator disc is defined as a function of the velocity across the disc by a local thrust coefficient  $c_x$  and so reasonable agreement may be expected. This is a little different from the experimental approach in which a discrete set of discs, each of different porosity, are selected to develop a discrete set of  $c_x$  values. However, the use of Equation 5 will be representative provided that the local thrust coefficient of a given disc does not vary significantly due to the small difference between Reynolds number of flow across the disc only and across the same disc within a duct. For the local thrust coefficient range  $0.5 < c_x < 10$  disc velocity is approx.  $0.9U_0 > U_D > 0.3U_0$  hence Reynolds number of flow relative to disc ( $\sim U_D D/\nu$ ) is  $135 \text{ k} > Re_D > 40 \text{ k}$ . Experimental data is available over this range (see Section 3) to select appropriate porosity for a small number of different  $c_x$  values of a bare disc. When located within a duct, the flow velocity across each disc reduces by up to 10% depending on  $c_x$  (see Figure 2.2). Experiments conducted with discs of different porosity at  $Re \sim 200 \text{ k}$  and  $Re \sim 40 \text{ k}$  indicate negligible variation of thrust coefficient over 10% change of  $Re$  (see Section 3.1).

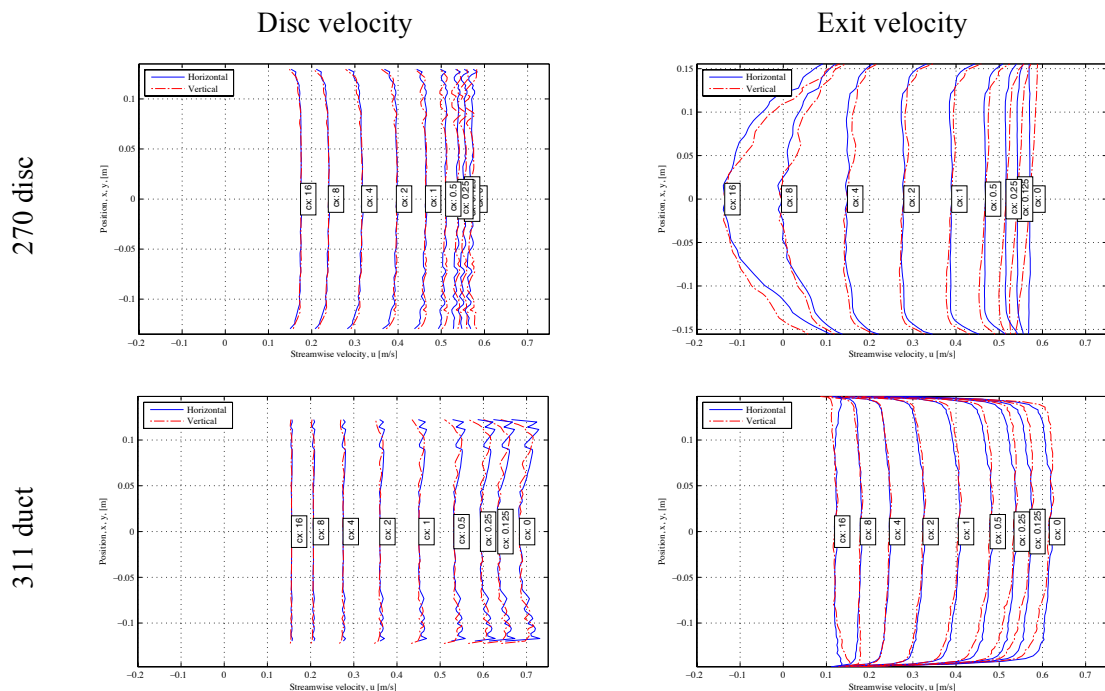
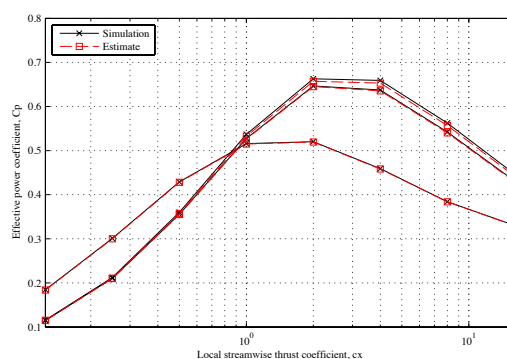


Figure 2.2: Radial variation of disc velocity (left) and velocity at  $X = L/2$  (right) for bare unducted discs of 270 mm and 311 mm diameter and disc of 270 mm diameter within 311 mm duct.





**Figure 2.3:** Power coefficient calculated by CFD simulation and estimated from force prediction by CFD simulation.

## 2.2 Rotor Performance: Low Blockage & Shear

Within PerAWaT experimental study of rotors has been conducted at two geometric scales: 1:30<sup>th</sup> approx. at EdF and 1:70<sup>th</sup> approx. at UoM. Both of these rotors were designed using GH Tidal Bladed assuming unconstrained flow. However, both sets of experiments are at relatively high blockage ratios and the rotor is within close proximity to bounding surfaces of both free surface and flume bed. Simulations have been conducted in WG3WP1 that show that both blockage and the presence of a sheared onset flow due to bed proximity alter turbine performance and wake structure. Experimental measurements of the WG4WP2 rotor at low blockage are required to increase confidence in the higher blockage 1:30<sup>th</sup> and 1:70<sup>th</sup> scale experiments conducted to date. This data will also increase confidence in interpretation of the turbine array results (1:70<sup>th</sup>) and their use within WG3WP4. These experiments comprise measurements of rotor performance only for three different locations within the water column (Table 2.2). Rotor angular speed, thrust and power must be measured to similar accuracy to WG4WP2.

- Important to understand how performance of a rotor is affected by blockage.
- Important to understand how performance of a rotor affected by shear profile of incident flow.

→ OUTPUT: Quantify CT(TSR) for UoM rotor at low blockage.

**Table 2.2x:** Test list for rotor performance at low blockage & sheared flow

Test No.	Hub height	TSR	Measurements			Velocity			
			<b>F<sub>x</sub></b>	<b>Ang.</b>	<b>τ</b>	<b>X</b>	<b>Y</b>	<b>Z</b>	<b>N<sub>U</sub></b>
2.1	-400	3 to 7	Y	Y	Y	2D	0	0	0
2.2	-200	3 to 7	Y	Y	Y	2D	0	0	0
2.3	-600	3 to 7	Y	Y	Y	2D	0	0	0

**Note:** see procedures section.

## 2.3 Rotor Wake: Bounding Surface Proximity

Experimental measurements of the effect of turbine position within the water column, including proximity to the free surface and bed, are required to further improve confidence in the general applicability of the PerAWaT wake models, particularly for use in the tool WG3WP4. Such data would complement the numerical investigations being conducted in WG3WP1D4 in which the

influence of vertical position within a shear profile is being modelled for a prototype scale rotor. The objective of these experiments is to characterise the influence of free surface proximity and a bed-generated shear layer on near wake structure ( $X < \sim 3D$ ) and far wake recovery of a rotor. As described in WG4WP2 the rotor must operate at a representative thrust coefficient and tip speed ratio and must impart swirl to the wake. All experiments will be conducted using the 270 mm rotor developed for WG4WP2 with torque constraint specified to attain a tip speed ratio  $TSR = 4.5$ . This operating point corresponds to maximum  $C_p$ .

**Table 2.3x:** Test list for rotor wake bounding surface proximity study

Test No.	Configuration		Measurements			Velocity Measurements			
	Hub height	TSR	Fx	Ang. Speed	$\tau$	X	Y-pos	Z-pos	$N_U$
3.11	-400	4.5	Y	Y	Y	1D, 3D, 5D,	0	0	6
						6D, 8D, 10D			
3.12						2D	0	ZptsB	16
3.13						4D	0	ZptsB	16
3.14						6D	0	ZptsA	8
3.15						2D	YptsA	0	7
3.16						4D	YptsA	0	7
3.17						6D	YptsA	0	7

3.21	-600	4.5	Y	Y	Y	1D, 3D, 5D,	0	0	6
						6D, 8D, 10D			
3.22						2D	0	ZptsC	17
3.23						4D	0	ZptsC	17
3.24						6D	0	ZptsD	11
3.25						2D	YptsA	0	7
3.26						4D	YptsA	0	7
3.27						6D	YptsA	0	7

3.31	-200	4.5	Y	Y	Y	1D, 3D, 5D,	0	0	6
						6D, 8D, 10D			
3.32						2D	0	ZptsC	17
3.33						4D	0	ZptsC	17
3.34						6D	0	ZptsD	11
3.35						2D	YptsA	0	7
3.36						4D	YptsA	0	7
3.37						6D	YptsA	0	7

**Note:** Velocity at each X,Y,Z ordinate to include 1 No. 5 min sample or 3 No. 1 min samples.

**Note:** co-ordinates for traverses Ypts-A, Zpts\_A-D are given in Appendix 3.

### 3 EQUIPMENT

#### 3.1 Flume

Experiments will be conducted in the EdF Channel as used for PerAWaT experiments on a 0.6 m diameter rotor, WG4WP1. The flow should be low turbulence to facilitate direct comparison with CFD. Water depth should be 0.8 m. Flow speed of greater than 0.45 m/s is required such that disc Reynolds number (i.e.  $U_0 D/\nu$ ) and blade Reynolds number of the rotor ( $\sim U_0(\text{TSR})/\nu$ ) are similar to the experiments of WG4WP2. In particular it is essential that the blade Reynolds number is of the order of 30 k or above since this governs the performance of the rotor (see WG4WP2D1-5). Flow speeds of 0.3 m/s and 0.55 m/s have been measured in the EdF flume at 0.8 m depth (see WG4WP1D3). For 0.3 m/s the flow is unidirectional, but for 0.55 m/s high velocity, lateral recirculation regions appear in the flume with velocity of the order of x% streamwise velocity. This flow, including the secondary lateral flows, have been modeled in CFD (WG3WP2) and will be of less significance for these experiments due to the smaller rotor diameter employed. Therefore low turbulence flow of 0.55 m/s will be employed.

#### 3.2 Disc Porosity and Geometry

Individual porous discs have been employed in numerous numerical studies and several experimental studies of tidal stream systems to represent the effect of energy extraction by a rotor. Assuming inviscid flow, Glauert showed that the resistance of a porous disc (here denoted  $k_n$ ) can be related to the thrust coefficient as  $C_T = 1/(k_n + k_n/4)^2$ . This resistance coefficient is not directly related to the geometry of the porous media. Geometric porosity is typically defined as the ratio of open area to solid (or closed) area  $K = A_{\text{OPEN}} / A_{\text{SOLID}}$  such that the total area of the disc is  $A = \frac{1}{4}\pi D^2 = A_{\text{OPEN}}(1+K)$ .

There is limited published information concerning the variation of thrust coefficient with geometric porosity of either discs or strips. Myers (2011) tested individual porous discs of 100 mm diameter and porosity 0.35 to 0.48 and report thrust coefficients in the range 0.61-0.94. Due to the limited information available to inform selection of disc porosity, experiments were conducted with isolated discs to quantify the variation of thrust coefficient ( $C_T$ ) with geometric porosity. These experiments were conducted using the flume, equipment and methods as detailed in WG4WP2D1-D5. Flow speed is  $U_0 = 0.46$  m/s, water depth  $h = 0.45$  m and disc diameter  $D=270$  mm. Reynolds number of the flow is 200k approx. and blockage is approx. 2.5% (single disc area / channel area =  $A_D/A_C = \frac{1}{4}\pi D^2/Wh$ ). Porosities  $0.2 < K < 1.6$  were manufactured by drilling holes of uniform diameter  $d = 10$  mm or 12 mm or 14 mm in 6 mm thick acrylic. Thrust coefficient ( $C_T$ ) is a nearly linear function of porosity (Figure 3.1). Note that, although discs with equal porosity develop equivalent thrust coefficient, the profile of axial velocity, i.e.  $U_x(Y,Z)$ , is dependent on the hole diameter and distribution within the disc area.

To select appropriate discs for experiments in a different flume, local thrust coefficient  $c_x$  is estimated on the basis of linear momentum actuator disc theory (LMADT) accounting for blockage (Figure 3.2). Disc porosities are selected (Table 2.1) to develop local thrust coefficients similar to 0.5, 1.0, 2.0 and 10.0 for discs of 270 mm diameter within the EdF flume of 1.5 m width and 0.8 m depth. As a consequence of increased blockage, thrust coefficient is slightly different to the present UoM experiments for equivalent local thrust.

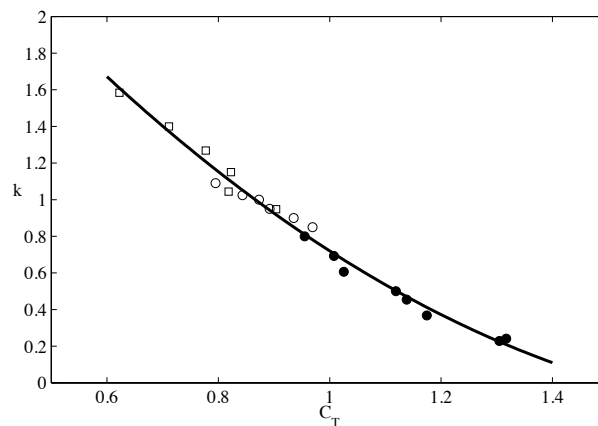


**Figure 2.1:** Variation of thrust coefficient with geometric porosity ( $k = A_{\text{OPEN}} / A_{\text{SOLID}}$ ) for range of hole diameters ( $d$ ). Data for  $Re \sim 225$  k and range of hole diameters. Trendline also shown.

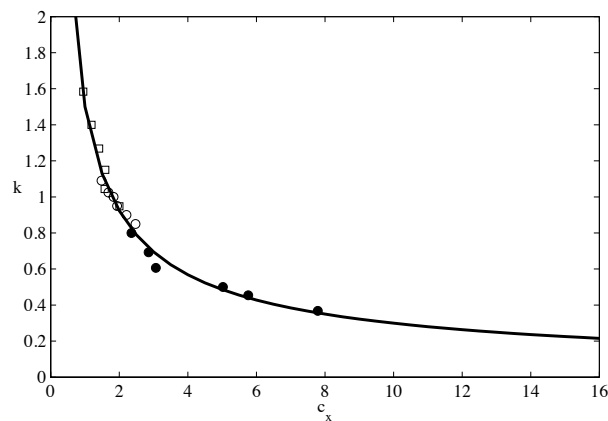


**Figure 3.2:** Variation of local thrust coefficient with geometric porosity ( $k = A_{\text{OPEN}} / A_{\text{SOLID}}$ ) for range of hole diameters ( $d$ ). Data for  $Re \sim 225$  k and range of hole diameters. Trendline also shown.

**Table 3.1:** Disc porosity  $k$  selected to attain specified local thrust coefficient  $c_x$  and corresponding global thrust coefficient for UoM and EdF flumes.

Diameter	270	270	270	270	270	311	311
$c_x$ , target	0.5	1.0	2.0	10.0	16	2.0	10.0
$c_x$ , experiment	0.6	0.9	1.8	10.0	16	1.8	10.0
$k$	<b>2.15</b>	<b>1.61</b>	<b>1.0</b>	<b>0.30</b>	<b>0.22</b>	<b>1.0</b>	<b>0.30</b>
$C_T$ , UoM flume	0.52	0.64	0.87	1.25	1.30	-	-
$C_T$ , EdF flume	0.45	0.60	0.88	1.28	1.33	-	-

Each of the discs listed in Table 3.1 are manufactured by drilling a pattern of holes from discs of 6 mm thick acrylic. The same approach was employed to obtain the measurements of Figure 3.2. The hole diameter, number and example pattern are summarised in Appendix A.

### 3.3 Duct Design

Duct shape ‘H’ as detailed by Fleming et al. (2011) with inner diameter 272 mm and outer diameter 311 mm. The inner diameter thus has 1 mm clearance to the circumference of the disc to allow for manufacturing tolerances and to facilitate installation and removal of the disc. The duct is manufactured from PA12-GF by the rapid prototyping method Selective Laser Sintering (SLS) as per rotors of WG4WP2. This process provides a direct reconstruction of the provided CAD geometry.

The duct is built in two parts (see Appendix B) that, when combined, form a single duct with circular hole in the top surface. This clamps around the 15 mm diameter support tower.

### 3.4 Thrust Measurement

Each strain-gauged structure is identical to the system described in WG4WP2D4 Section 4.1 and comprises a 15 mm outer diameter stainless steel tube with 1 mm (approx.) wall thickness. Strain gauges are surface mounted 800 mm above the rotor and disc axis. Each strain gauge is calibrated prior to test by application of fixed increment masses and a linear relationship is obtained between applied moment and measured voltage (method as WG4WP2D4). The UoM support structure is connected to the EdF gantry mounting plate that has 4 No. 8 mm diameter holes on a radius of 180 mm. Three no. structures have been designed for this purpose to support the disc centre and rotor axis at immersion depths of 200 mm, 400 mm and 600 mm.

### 3.5 Rotor Torque and Speed Measurement

The rotor and mechanical system is identical to the system described in WG4 WP2 D5. The rotor is mounted directly on the shaft of a 90o bevel gearbox with acrylic gears (REF) (FIGURE). The gearbox is mounted on a 15 mm outer diameter stainless steel rod with strain gauges located XXX mm from hub centreline. Only the rotor, gearbox and lower part of supporting shaft are immersed. This configuration was chosen rather than an immersed nacelle to minimize dimensions of the immersed support structure enabling velocity measurement to within 0.4D downstream of the rotor plane. Retarding torque,  $\tau_m$ , is applied to the rotor by a dynamometer system developed by Brown [Brown 2008] and described by Weller et al. [Weller 2010]. This comprises a firmware controller that specifies the bridge current across a CROUZET 82800 series 24 VDC motor as a function of measured angular speed. Angular displacement is measured using a HEDS 9000 quadrature encoder reading an HEDM 6120 T12 code wheel. The code-wheel has 2000 counts per revolution thus providing position to  $\pi/100$ . Angular speed,  $\omega_m$ , is obtained by differentiation of the measured angular displacement. Rack of min 4 control cards to be taken to EdF.

### 3.6 Flow Measurement

**Incident velocity** for the selected flow (see Section 3.1) is detailed in WG4WP1D1.

**Wake velocity** only is measured during these experiments. The main interest is A Nortek Vectrino sampling at 25 Hz is employed (as used in WG4 WP1). The probe head is downwards pointing such that:

- EdF ADV x-axis aligned with flume X-axis
- EdF ADV y-axis aligned with flume Y-axis
- EdF ADV z-axis aligned with flume Z-axis

A second measurement device is also available for use during the experiments if necessary. This is a NORTEK Vectrino+ ADV (as used by UoM in WG4 WP2) sampling at up to 200 Hz with a support rod and clamp to mount the probe head horizontally such that:

- ADV x-axis aligned with flume X-axis.
- ADV y-axis aligned with flume Z-axis.
- ADV z-axis aligned with flume Y-axis.

Repositioning between measurement locations will be a manual process. Designs for an automated vertical traverse system were developed prior to start of WG4WP3. This would allow measurement of flow velocity at a larger number of points than a manual repositioning system during the test programme since manual intervention would be reduced. However, the manufacturing time for this device was not sufficiently well defined to guarantee availability for the experiments. Therefore, the proposed series of experiments is designed to allow for manual repositioning of the ADV.

### 3.7 Data Logging

All data to be recorded to a dated directory in the first instance and subsequently *copied* to a directory for corresponding test number when collection completed. Wake velocity measurements will be recorded with either EdF or UoM ADV sampling at min 25 Hz. Prior to commencing wake velocity measurements on each date, min 1 min sample of Signal to Noise Ratio (SNR) and Correlation Coefficient (COR) should be recorded. Acceptable levels for testing are SNR > 15 dB and COR > 90%. Velocity time history files to be provided with measurement co-ordinates defined in filename, e.g.:

Uxyz\_Xxpt\_Yypt\_Zzpt.fff

Where *xpt*, *ypt* and *zpt* the measurement location (in mm) relative to an origin at *xpt* = 000 at the rotor plane, *ypt* = 000 on flume bed and *zpt* = 000 flume centreline. File format (fff) should be either ascii (\*.dat) or, when Nortek software employed, both Nortek binary format (\*.nor) and converted ascii formats (\*.vel, \*.snr, \*.cor).

Mechanical parameters will be recorded direct from the UoM dynamometer employing a National Instruments Labview interface similar to the system described in WG4WP2D3. Data sampled at 200 Hz. A National Instruments 6211-USB input card will be employed with the pin configuration as listed in Table 3.2.

**Table 3.2:** Device pinouts for NI 6211-USB data logging interface.

AI0	Voltage	ADV Ux	UoM ADV only
AI1	Voltage	ADV Uy	UoM ADV only
AI2	Voltage	ADV Ux	UoM ADV only
AI3	Voltage	ADV Uz'	UoM ADV only
CTR1	Digital count	Angular position	Rotor only
<b>AI4</b>	<b>Voltage</b>	<b>Strain Gauge</b>	<b>All tests</b>
AI5	Voltage	Proportional to mechanical torque	Rotor only

A single ascii format output file is generated containing synchronised time-history of all measured parameters. After positioning of the equipment required for each test and prior to commencing mechanical parameter measurement, min 3 No. 1 min samples should be recorded with zero flow speed to provide a zero offset datum. Filename should be:

ZeroSet\_TestNo\_A.dat

During multi-point wake studies, (test series 1 and 3) mechanical parameter time-history files to be recorded with reference to the co-ordinates of the measurement volume within the wake, e.g.:

Data\_Xxpt\_Yypt\_Zzpt.dat

During rotor load studies (test series 2 only), mechanical parameter time-history files to be recorded with reference to the applied value of Igen, e.g.:

Data\_Igen.dat

Note: ascii files (e.g. \*.dat) must not be *opened* directly into Excel at any time.

## 4 LOGISTICS

Equipment required all tests and for each series of tests is given in Section 4.1.

### 4.1 Equipment to dispatch to EdF

- **Equipment for all tests**

15 m dynamometer OUTPUT cable (x2)	Available
PC	At EdF
Power lead + EU adapter plug (x2)	Available
Strain gauge calibration equipment	Available
Labview routines on USB HDD	Collate and send
Nortek Vectrino+ software on USB HDD	Available
Nortek Polysync on USB HDD	Available
G-clamps	Available
Tools	Available
Hard Disk	Available

- **Equipment for Test Series 1: measure and log thrust on disc and disc + duct**

UoM to EdF clamp for 400 mm hub height	Due 20 Sep 12 at UoM
Disc support Structure with rigid mounting pin	Available
Splitter cable from PerAWaT dynamometer OUTPUT to NI pins	Available
USB NI interface (velocity and strain only: voltages)	Available
Discs (5 No. 270 mm)	Due 18 Sep 12 at UoM
Discs (2 No. 311 mm)	Due 18 Sep 12 at UoM
Duct (1 No.)	Delivery to UoM 18 Sep 12

- **Equipment for Test Series 2 and 3: measure and log rotor**

UoM to EdF clamp for 400 mm hub height	Manufacture
UoM to EdF clamp for 200 mm hub height	Manufacture
UoM to EdF clamp for 600 mm hub height	Manufacture
PerAWaT dynamometer & rotor support structure	Available
PerAWaT dynamometer power supply (x1 rack)	Available
Splitter cable from PerAWaT dynamometer OUTPUT to NI pins (Table 3.7)	Available
USB NI interface (velocity, strain & ang. Speed: voltages & digital)	Delivered to UoM 12 Sep 12
Rotor (x1)	Available

- **Additional Equipment**

Laptop	UoM to source spare
Vectrino+ ADV inc. Probe, tools, RS232 to USB.	Available
Vectrino+ sideways probe on 1 m cable	Available
Mounting rod for Vectrino	Available
Rotor spare (x1, metal rotor)	Delivered to UoM 12 Sep 12

## 4.2 Indicative Schedule of Experiments

The following sequence of activities is proposed for the experimental campaign at EdF Chatou. Note that the total test duration is expected to be approximately 22 days during an eight-week period. Thus tests will not necessarily be conducted continuously. If any issues arise several days of adjustment to the schedule are possible. All experiments will be conducted by EdF staff. However, UoM staff will be on-site to witness tests and for technical discussion before all tests and during some tests. It is estimated that there will be three visits by UoM to EdF Chatou up to end November 2012.

**UoM visit 1:** Explain equipment and processes

**UoM visit 2:** Review test series 1 and preparations for test series 2.

**UoM visit 3:** Review test series 2.1,2.2 and 3.11-3.27 and final preparations.

UoM	Experiment Stage	Duration of flume use (Estimated)
Visit 1	Initial meeting and equipment setup	
	Connect disc support structure to logging system, check and calibrate thrust	
	Tests 1.11-1.17          270 mm discs → 8 tests, 66 wake points	~ 4 days
	Tests 1.31-1.32          311 mm discs → 2 tests, 16 wake points	~ 1 day
	Tests 1.21-1.28          DUCTED → 9 tests, 67 wake points	~ 4 days
Visit 2	Review initial data	
	Connect rotor support structure to logging system, check and calibrate thrust	
	Tests 2.1                  270 mm rotor → CT(TSR)	~ 1 day
	Test 3.11-3.17 → 8 wake studies over 67 wake points	~ 3 days
	Connect UoM-EdF clamp for hub height -600 mm: near bed	
	Tests 2.2 and Tests 3.21-3.27 → CT(TSR) → 8 wake studies comprising 72 wake points	~ 4 days
Visit 3	Review data to-date.	
	Connect UoM-EdF clamp for hub height -200 mm: near surface	
	Tests 2.2 and Tests 3.21-3.27 → CT(TSR) → 8 wake studies comprising 72 wake points	~ 4 days

**This schedule is preliminary and will be adjusted if necessary to deliver the required data.**



## 5 CONCLUSIONS

This report details the design and specification of a series of experiments to provide i) direct comparison of the performance of an unducted turbine and ducted turbine, ii) increase understanding of the effect of bounding surface proximity on rotor performance and wake structure. All experiments will be conducted at the EdF facility Channel 5 with section depth 0.8 m and width 1.5 m. Disc diameters of 270 mm and 311 mm, duct outer diameter of 311 mm and rotor of diameter 270 mm are employed such that blockage is of the order of 4.8 – 6.3%. The low turbulence flow case with mean velocity  $U_0 \sim 0.55$  m/s will be employed as characterised in WG4 WP1 D1. This flow velocity is similar to the flow-speed employed for rotor experiments in WG4WP2 and disc experiments in WG4WP4 hence equipment and data obtained using those studies is used both directly and to inform design.

CFD simulations are presented of two actuator discs of diameter equal to the inner and outer diameter of a duct. Both discs develop similar effective power over the range of local thrust coefficients considered. Effective power coefficient is slightly increased by duct augmentation for small values of local thrust coefficient ( $c_x < \sim 1$ ) but is significantly reduced for higher values of local thrust coefficient. Discs are designed to obtain direct comparison of unducted and ducted performance at five thrust coefficients. Measurements are required of both thrust force and nearwake velocity at specified co-ordinates to obtain data suitable for comparison to CFD predictions of performance.

Rotor experiments employ identical equipment to the experiments of WG4WP2. Thrust on the rotor blades will be greater than previous experiments and so a spare, metal, rotor has been manufactured for these experiments. A connection has been manufactured to provide a rigid connection between the rotor support structure and EdF flume gantry. Rotor thrust and angular speed will be measured for a range of mechanical torque to determine the variation of thrust coefficient with tip speed ratio. Specific wake measurement points are defined to obtain insight into the effect of bounding surface proximity on wake structure. Time constraints precluded the development of an automated traverse system similar to the system used in WG4 WP2. Thus, the wake measurement points have been selected so that the test programme can be completed with manual repositioning of the velocity measurement device.

Equipment required for all experiments, and for each series of experiments, has been identified and, where necessary, designed and manufactured. All items required for the first series of experiments are available for dispatch from UoM to EdF. Delivery is awaited of some items required for experiments of series 2 and 3. This is expected by end September and will be dispatched to EdF when available. Equipment for all tests, spares and equipment for test series 1 will be dispatched by UoM to EdF during week of 17<sup>th</sup> September 2012. Subject to travel arrangements, UoM staff will visit EdF Chatou to assist with equipment setup during last week of September 2012 or first week October 2012. EdF has confirmed availability of Channel 5 for these experiments up to end November 2012 (VM/P74/2012/25) and that experiments will be conducted by EdF staff in accordance with health & safety procedures developed for this facility (VM/P74/2012/25). It is therefore expected that the test programme will be completed and quality controlled data delivered to UoM, GH and UoO by end November 2012 as required for WG4 WP3 D2.

## REFERENCES

- Myers, L.E. and Bahaj, A.S. An experimental investigation simulating flow effects in first generation marine current energy converter arrays. *Renewable Energy* 37 (2012) 28-36.
- Stallard, T.J. Thomson, M., Collings, R., and Whelan, J, Calibration report for Scale Model Experiments. ETI PerAWAT WG4 WP2 D4, Feb 2011.
- Thomson, M., Collings, R., Stallard, T. and Feng, T. Summary of findings from scale model study of an array of tidal stream rotors. ETI PerAWAT WG4 WP2 D5, Jun 2011.
- Fleming, C.F., McIntosh, S.C. and Willden, R.H.J. Design and Analysis of a Bi-Directional Ducted Tidal Turbine. In Proc 8<sup>th</sup> EWTEC. Sep 2011, Southampton, UK.

## APPENDIX 1: POROUS DISC DESIGNS

Seven No. discs have been manufactured with sufficient number of holes to develop the porosity values listed in Table 3.1. A summary of hole diameter and number for each disc is given below and example of hole pattern of discs 2 and 7 given below:

No.	1	2	3	4	5	6	7
Disc diameter	270	270	270	270	270	311	311
Hole diameter	12	12	12	12	12	12	12
Number holes	346	312	254	117	91	336	155
$k = A_{\text{open}} / A_{\text{solid}}$	<b>2.15</b>	<b>1.61</b>	<b>1.0</b>	<b>0.30</b>	<b>0.22</b>	<b>1.0</b>	<b>0.30</b>

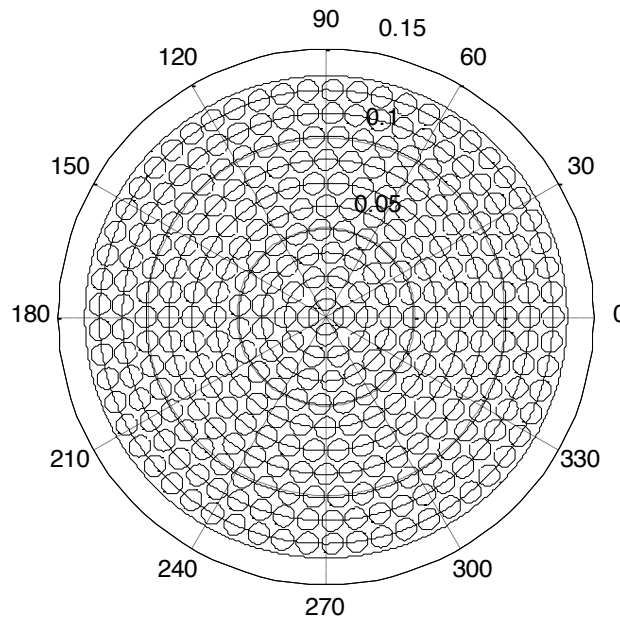
### Disc 2

Material 6mm PVC

Disc Diameter: 270mm

4mm hole in the centre of disc.

Holes in total: 312, porosity=1.6062



Cycle Radius (mm)	Holes on the Cycle
10	4
23	10
36	17
49	23
62	28
75	34
88	40
101	46
114	53
127	57

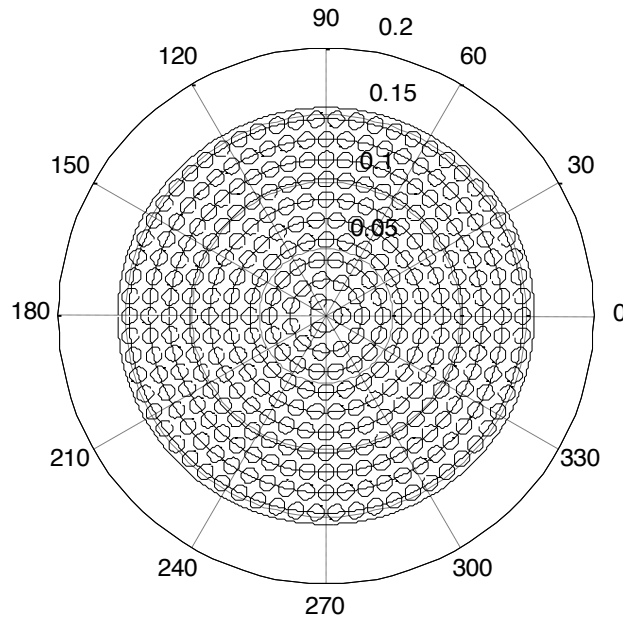
**Disc 6**

Material 6mm PVC

Disc Diameter: 311mm

Drill a 4mm hole in the centre of disc.

Holes in total: 336, porosity=1.001

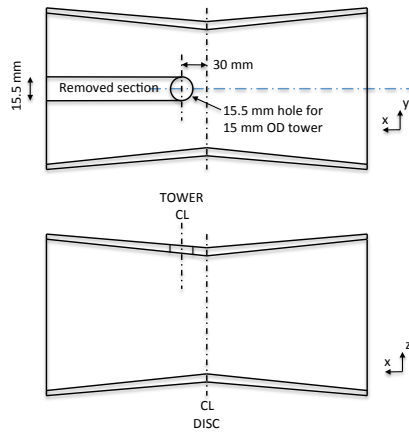


Cycle Radius (mm)	Holes on the Cycle
12	3
27	11
42	18
57	24
72	30
87	36
102	44
117	52
132	56
147	62

**APPENDIX 2: DUCT DESIGN**

The duct geometry is defined by Fleming et al. (2011) with internal diameter 272 mm and external diameter 311 mm. The duct is manufactured in two parts from CAD files of two components as sketched in Figure A2.

FILE1: DUCT\_dext311\_dint272\_v2.stp



FILE2: DUCT\_dext311\_dint272\_infill.stp

Infill Section to install when duct attached to tower & disc



Figure A2: Two parts of duct CAD.

### APPENDIX 3: WAKE MEASUREMENT CO-ORDINATES

With reference to Tables 2.1 and 2.3 the following traverse co-ordinates are required.

#### DISC TRAVERSE, DUCT TRAVERSE

Ypts-A		Ypts-B	
Nu=		Nu=	
Y	Z	Y	Z
-60	0		
20	0		
60	0	60	0
100	0	120	0
140	0	150	0
180	0	180	0
240	0		

#### ROTOR at Z = -400 mm

Zpts-A	
Nu=	
Y	Z
0	-60
0	0
0	20
0	60
0	100
0	140
0	180
0	240

Zpts-B	
Nu=	
Y	Z
0	-240
0	-180
0	-160
0	-140
0	-120
0	-80
0	-40
0	0
0	40
0	80
0	120
0	140
0	160
0	180
0	240

#### ROTOR at Z = -600 mm and -200 mm

Zpts-C		Zpts-D	
Nu=		Nu=	
Y	Z	Y	Z
0	-160	0	-160
0	-145	0	-145
0	-130	0	-130
0	-115		
0	-100	0	-100
0	-60	0	-60
0	-20		
0	0	0	0
0	20		
0	60	0	60
0	100	0	100
0	120		
0	140	0	140
0	160		
0	180	0	180
0	240		
0	280	0	280